Supplementary Material

Treatment Planning

Clinical Treatment Planning

The clinical treatment plans were generated for delivery on PSI Gantry 2 using the in-house developed treatment planning system 'PSIplan' [1,2]. Candidate proton spots were placed on a regular grid with 4 mm lateral spacing and 2.5 mm spacing between energy layers, covering the planning target volume (PTV) expanded by an additional 5 mm. Due to the superficial location of the sinonasal tumors, a 42 mm (water-equivalent) pre-absorber was used for all fields, resulting in spot widths ranging from 16.9–3.7 mm (sigma in-air at isocenter), for proton energies of 73–229 MeV. Candidate spots from all four fields were optimized simultaneously in a multi-field optimization approach and spots below a minimum weight of approximately $0.5*10^6$ protons per fraction were excluded from the plan. The conventional clinical treatment planning process is schematically illustrated in Figure S1.

Spot-reduced Treatment Planning

Spot-reduced treatment plans were generated using a research treatment planning system, based on the open-source toolkit 'matRad' [3] with in-house developed extensions for intensity-modulated proton therapy (IMPT) optimization. The system uses the so-called 'pencil beam resampling' paradigm [4]. This means that the IMPT optimization is performed repeatedly in an iterative process, instead of the traditional approach in which candidate spots are optimized all together in a single optimization run. Each 'resampling iteration' consists of: 1) random selection of a small subset of candidate spots which are added to the existing solution of the previous resampling iteration (note that in the first iteration an existing solution is not available yet), 2) dose optimization, and 3) spot reduction. The dose

optimization is performed according to a prioritized (or 'lexicographic') multi-criteria approach, in which the planning objectives are optimized one-by-one according to their user-defined priority, while constraining previously obtained objectives with a higher priority [5]. This allows for fully automated generation of high-quality treatment plans [6]. Each resampling iteration is concluded by the iterative exclusion of low-weighted spots from the plan (i.e. below a minimum spot weight of $1.0*10^6$ protons per fraction and/or within the 0.5%-percentile of cumulative spot weights), during which all previously achieved planning objectives are constrained and the weights of the remaining spots are reoptimized. Spot reduction is continued until a feasible solution can no longer be achieved without violating these constraints. The resampling iterations are terminated when either all planning objectives have been achieved or when none of the objectives improves more than 3%. A flow-chart of the pencil beam resampling planning process is shown in Figure S1, together with a schematic illustration of traditional planning as a reference. In the current study, we used a total sample size of 5,000 spots (over all fields) per iteration, which were randomly sampled from a grid similar to the clinical spot grid (i.e. target definition, energy spacing and pre-absorber), but with a finer lateral spacing of 1 mm. The beam model of PSI Gantry 2 used for clinical treatment plan generation was also used during spot-reduced treatment planning. In this study, after obtaining the spot-reduced treatment plan, we performed a single final optimization run in which the lowest spot weight was maximized while constraining all dose objectives. An experimental validation of the deliverability, accuracy and robustness of such a spot-reduced treatment plan has previously been performed at our institute [7].

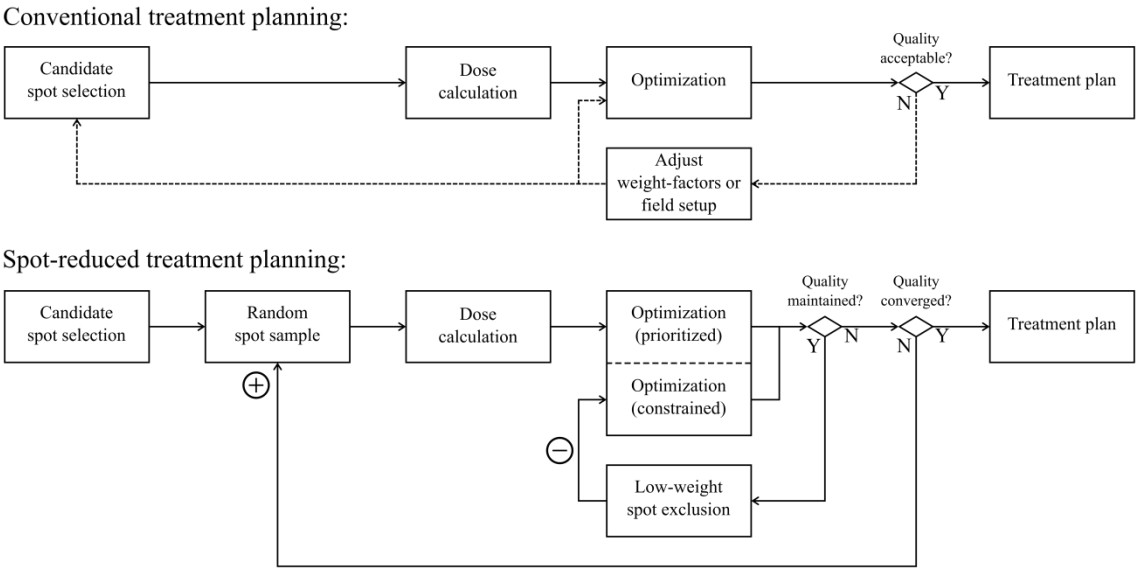

Figure S1. Flow-charts of the conventional and spot-reduced treatment planning process. Dashed arrows indicate manual interventions by the user.

Beam Intensity

Figure S2 shows the beam intensity (in protons/s) at isocenter as a function of proton energy. The solid lines indicate the current clinical machine characteristics, with the constant beam intensity on PSI Gantry 2 in red, and the maximum achievable variable beam intensity on PSI Gantry 3 in blue. To limit the variation in beam intensity with energy and to ensure patient safety, the maximum clinical beam intensity on PSI Gantry 3 is intentionally restricted for proton energies above 169 MeV, whereas increased cyclotron output (>800 nA) can be requested for energies below 110 MeV if the accelerator permits. The dashed blue line indicates the theoretically achievable maximum beam intensity on PSI Gantry 3, based on representative transmission data that was obtained by Monte-Carlo beamline simulations [8] and by gantry measurements, while considering a realistic 800 nA beam current at the cyclotron [9].

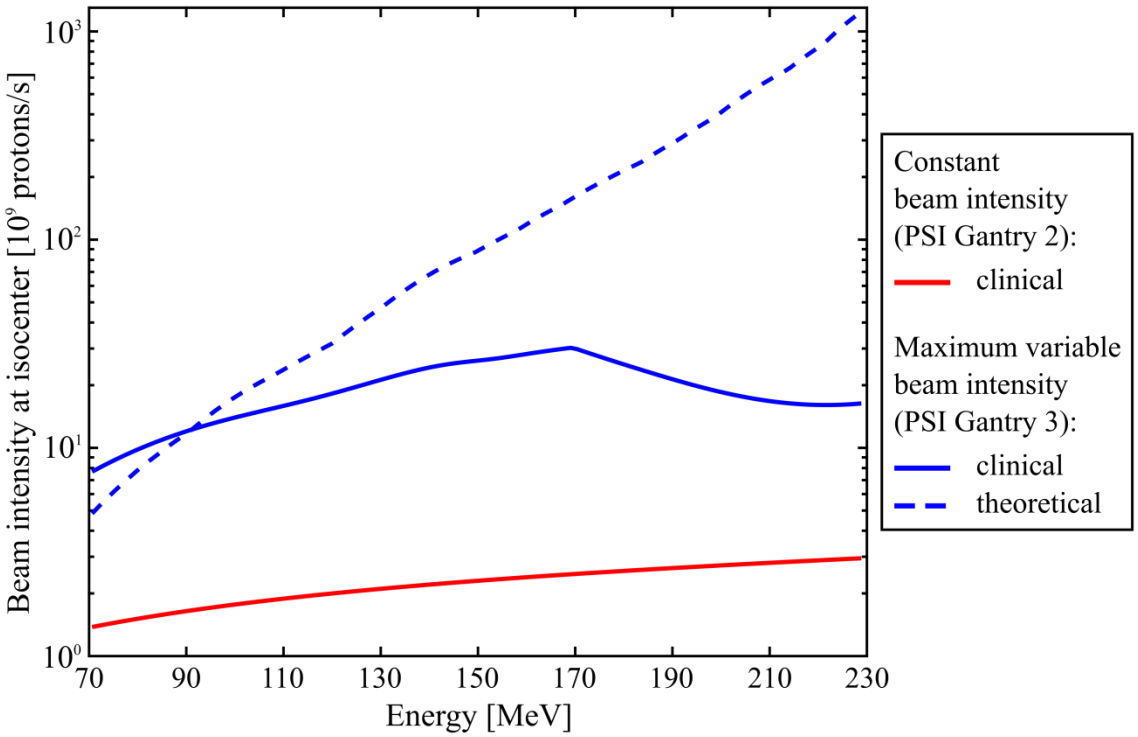

Figure S2. Constant beam intensity at isocenter on PSI Gantry 2 (in red) and maximum available variable beam intensity at isocenter on PSI Gantry 3 (in blue; solid: clinical; dashed: theoretical) as function of proton energy.

Dose-averaged Dose Rate Distributions for simple Cases and clinical Delivery

In this study, we introduced the new 'dose-averaged dose rate' (DADR) metric. To provide a reference when interpreting the DADR distributions presented in this paper, we additionally performed DADR calculations for two simple cases. Figure S3 shows the dose distributions and DADR distributions for a square phantom with a single field and for patient 1 with a single lateral shoot-through spot-reduced field, in addition to the clinical treatment plan of patient 1. The square phantom contained a 50x50x50 mm target volume located at a water-equivalent depth ranging between 176–224 mm, for which we used a single field with proton energies of 157–186 MeV (no pre-absorber), optimized using conventional (non-spot-reduced) treatment planning. The DADR distributions depicted in Figure S3 were calculated

for the extreme delivery scenarios: constant beam intensities (PSI Gantry 2) with 2 Gy fraction dose (which corresponds to the actual delivery of the clinical treatment plan) and theoretical spot-wise variable beam intensities (PSI Gantry 3) with 6 Gy fraction dose.

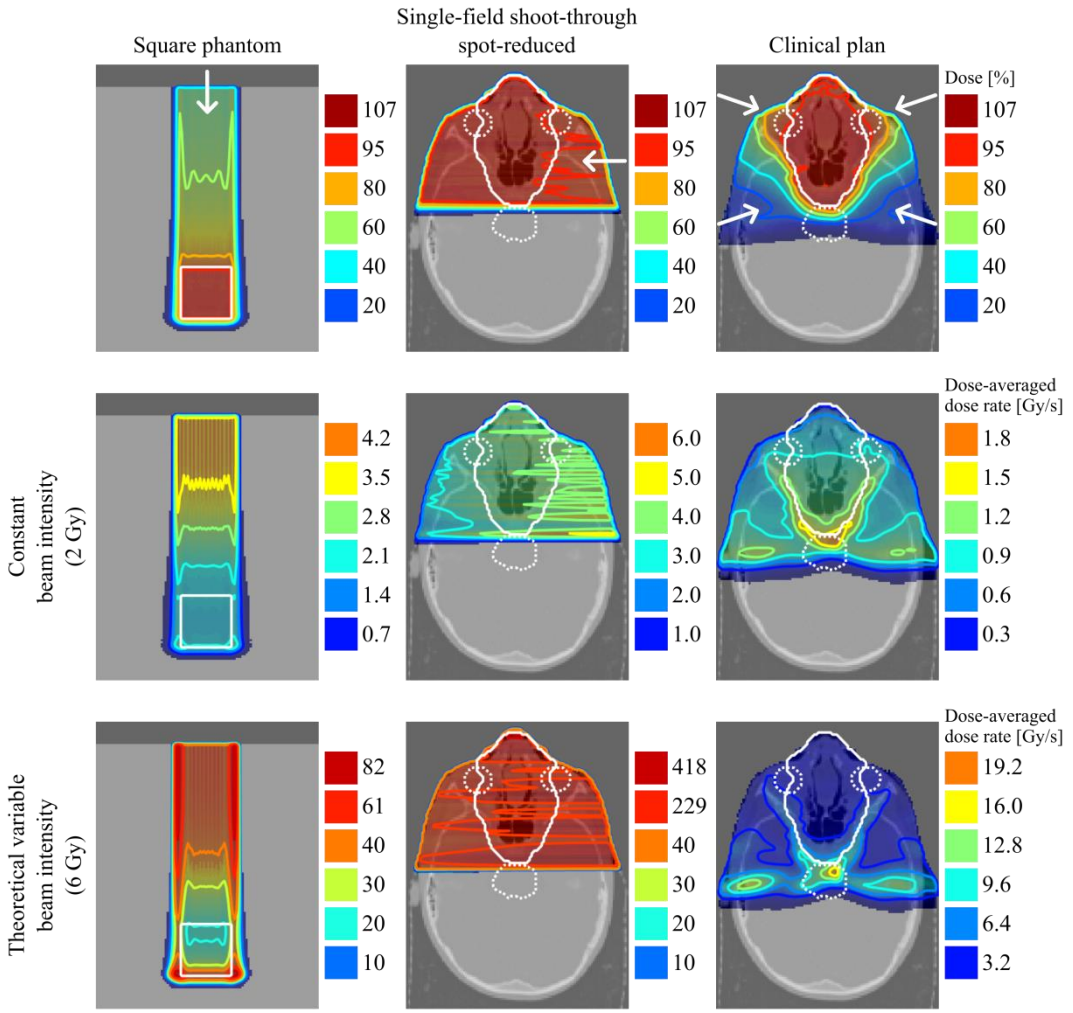

Figure S3. Dose distributions (top row) and dose-averaged dose rate distributions (bottom rows) for a square phantom with a single field (left column), patient 1 with a single shoot-through field (middle column), and the clinical treatment plan for patient 1 (right column). Constant beam intensity on PSI Gantry 2 with 2 Gy fraction dose (middle row) and theoretical spot-wise variable beam intensity on PSI Gantry 3 with 6 Gy fraction dose (bottom row) were assumed. White contours indicate the PTV (solid), and eyes and brainstem (dotted). White arrows indicate the applied field directions.

Delivery Time-Structure

The delivered dose per spot in randomly selected voxels is depicted in Figure S4 for the different treatment plans of patient 1. We sampled voxels that received a total dose of approximately 2.0, 1.0 and 0.5 Gy located in the planning target volume (PTV, only for 2.0 Gy) or the normal tissue, and for which we found high dose-averaged dose rates above the FLASH threshold (>40 Gy/s) or within 10% of the maximum dose rate value, when assuming the hypofractionated theoretical variable beam intensity delivery scenario. To avoid making assumptions regarding the delivery dynamics of a specific spot-scanning proton machine, the delivered dose was plotted as function of the spot number, with the spots sorted according to the anticipated order of delivery. The figure shows that, especially for the spot-reduced treatment plans and for lower total voxel dose, most of the dose in these voxels was delivered by a limited number of proton spots. Moreover, the figure indicates that the timing of dose delivery (e.g. spread out over entire fraction or condensed within a limited time frame) could differ greatly between the different voxels and treatment plans.

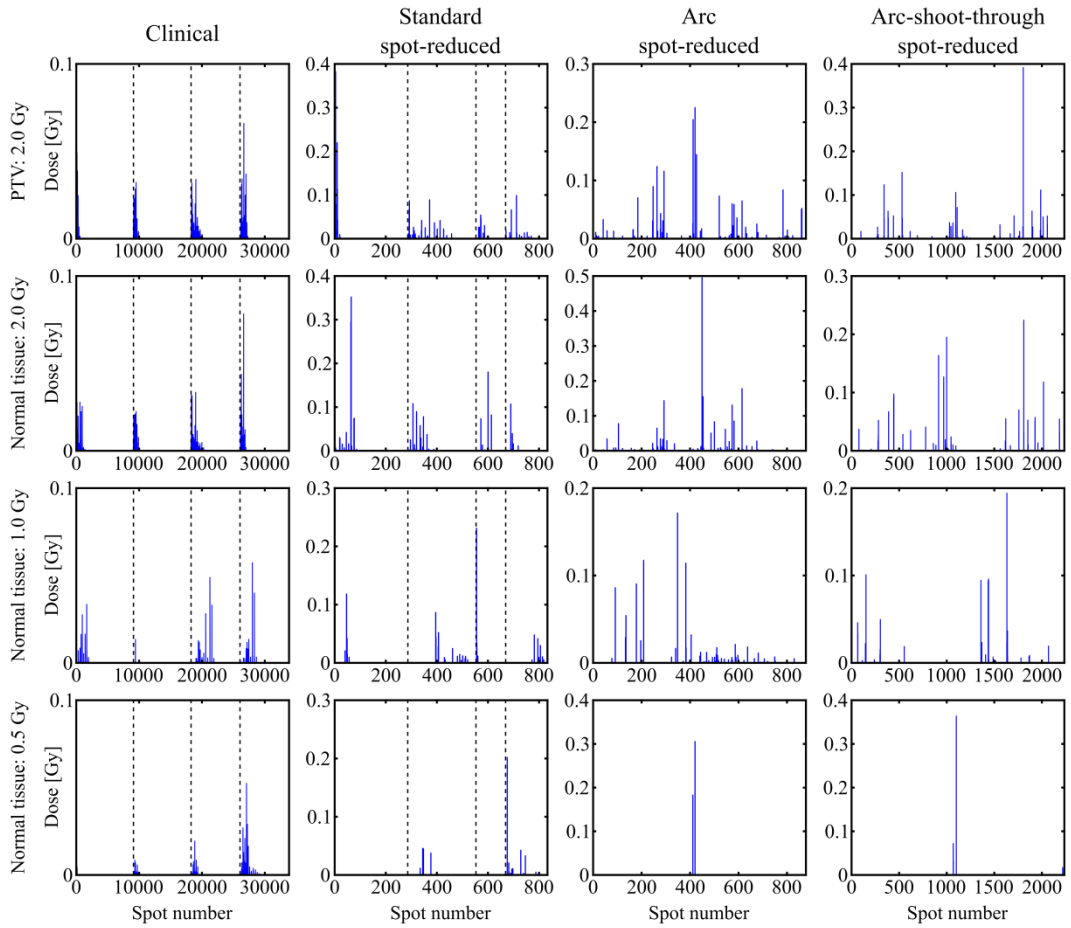

Figure S4. Delivery time-structure for the treatment plans of patient 1. The delivered dose per spot is depicted for randomly selected voxels in the PTV and normal tissue receiving 2.0, 1.0 or 0.5 Gy, with dose-averaged dose rates above 40 Gy/s or within 10% of the maximum dose rate when assuming the hypofractionated theoretical delivery scenario. The spot number reflects the expected order of delivery. Dashed lines indicate the individual (four) fields for the non-arc treatment plans.

References

[1] Lomax A. Intensity modulation methods for proton radiotherapy. Phys Med Biol. 1999;44:185–205.

[2] Lomax AJ, Böhringer T, Bolsi A, et al. Treatment planning and verification of proton therapy using spot scanning: Initial experiences. Med Phys. 2004;31:3150–3157.

[3] Wieser H-P, Cisternas E, Wahl N, et al. Development of the open-source dose calculation and optimization toolkit matRad. Med Phys. 2017;2556–2568.

[4] van de Water S, Kraan AC, Breedveld S, et al. Improved efficiency of multi-criteria IMPT treatment planning using iterative resampling of randomly placed pencil beams. Phys Med Biol. 2013;58:6969–6983.

[5] Breedveld S, Storchi PRM, Voet PWJ, et al. iCycle: Integrated, multicriterial beam angle, and profile optimization for generation of coplanar and noncoplanar IMRT plans. Med Phys. 2012;39:951–963.

[6] Voet PWJ, Dirkx MLP, Breedveld S, et al. Toward Fully Automated Multicriterial Plan Generation: A Prospective Clinical Study. Int J Radiat Oncol Biol Phys. 2013;85:866–872.

[7] Belosi MF, Water SV de, Albertini F, et al. PO-0894: Reduced spot number for PBS proton therapy shortens delivery time without dosimetric plan compromise. Radiother Oncol. 2018;127:S474–S475.

[8] Goethem MJ van, Meer R van der, Reist HW, et al. Geant4 simulations of proton beam transport through a carbon or beryllium degrader and following a beam line. Phys Med Biol. 2009;54:5831–5846.

[9] Rizzoglio V, Adelmann A, Baumgarten C, et al. Evolution of a beam dynamics model for the transport line in a proton therapy facility. Phys Rev Accel Beams. 2017;20:124702.